Conf-900936--26

Interactions of Energetic Particles and Clusters with Solids*

CONF-900936--26

DE91 006584

R. S. Averback, Horngming Hsieh
University of Illinois-Urbana
Urbana, IL 61801

T. Diaz de la Rubia
Lawrence Livermore National Laboratory
Livermore, CA 94550

and

R. Benedek
Argonne National Laboratory
Materials Science Division
Argonne, IL 60439

DECEMBER 1990

INVITED PAPER: Submitted to IBMM-90 Conference, Knoxville, TN, September 10-14, 1990. To be published in Nucl. Instr. and Meth. B.

* Work Supported by the U.S. Department of Energy, BES-Materials Sciences, under Contract W-31-109-ENG-38.

INTERACTIONS OF ENERGETIC PARTICLES AND CLUSTERS WITH SOLIDS

R.S. Averback[1], T. Diaz de la Rubia[2], Horngming Hsieh[1] and R. Benedek[3]

[1]Department of Materials Science and Engineering, University of Illinois at Urbana-Champaign Urbana, IL. 61801

[2]Chemistry Division, Lawrence Livermore National Laboratory, Livermore, CA. 94550

[3]Materials Science Division, Argonne National Laboratory, Argonne, IL. 60439

ABSTRACT

Ion beams are being applied for surface modifications of materials in a variety of different ways: ion implantation, ion beam mixing, sputtering, and particle or cluster beam-assisted deposition. Fundamental to all of these processes is the deposition of a large amount of energy, generally some keV's, in a localized area. This can lead to the production of defects, atomic mixing, disordering and in some cases, amorphization. Recent results of molecular dynamics computer simulations of energetic displacement cascades in Cu and Ni with energies up to 5 keV suggest that thermal spikes play an important role in these processes. Specifically, it will be shown that many aspects of defect production, atomic mixing and "cascade collapse" can be understood as a consequence of local melting of the cascade core. Included in this discussion will be the possible role of electron-phonon coupling in thermal spike dynamics. The interaction of energetic clusters of atoms with solid surfaces has also been studied by molecular dynamics simulations. This process is of interest because a large amount of energy can be deposited in a small region and possibly without creating point defects in the substrate or implanting cluster atoms. The simulations reveal that the dynamics of the collision process are strongly dependent on cluster size and energy. Different regimes where defect production, local melting and plastic flow dominate will be discussed.

1. INTRODUCTION

The interactions between energetic particles and solids has been a focus of research for many years. Initially this work was motivated by the need to characterize radiation effects in reactor components, and although many fundamental questions still remain in this field, most current work on ion-solid interactions has been focused on the use of ion beams for materials modification and thin film growth applications. Despite the prolonged interest in atomic collisions in solids, developing a satisfactory theoretical model for this phenomenon

has been difficult because the collision cascade that is produced by energetic ions is generally nonlinear, spatially inhomogeneous and involves many body interactions. As a first approximation, one can treat the short-time ballistic phase of the cascade evolution, when particle energies are high and the density of moving atoms is small, using the approximations of binary collisions and linear interactions (i.e., moving atoms meet only stationary atoms) [1-3] and the later stages, when the local region has thermalized, by a combination of classical heat transport equations and chemical rate theory [4-6]. This procedure has been useful in providing a qualitative understanding of various aspects of cascade phenomena, but it has not, in general, proved quantitatively reliable. Consequently, detailed understanding of various cascade phenomena has remained elusive.

In recent years, molecular dynamics (MD) computer simulations has emerged as a practical tool for studying the entire history of a cascade event. The suitability of this technique for radiation damage problems was originally recognized by Vineyard and co-workers as discussed in their classic paper of thirty years ago [7]. Although limited computer capabilities in those days restricted simulations to collision events under ≈ 400 eV, those pioneering studies demonstrated the enormous power of of MD for elucidating dynamic processes in energetic displacement cascades. With present generation supercomputers, it is now possible to simulate collision events with energies approaching 25 -50 keV and with far more realistic interatomic potentials [8]. Our work in this field has concentrated on two problems, the dynamics of energetic displacement cascades and cluster-solid interactions. Much of our work on the former can now be found in the literature [9-12], and it will be only briefly reviewed here. Emphasis will rather be placed on the consequences of our results for various radiation effects and new studies at higher energies [8]. In addition, the interaction of energetic (keV) clusters of atoms with surfaces will also be discussed. Although the importance of clusters in the so called "ionized cluster beam" deposition process[13] has recently been questioned [14], understanding the interaction of energetic clusters with solid substrates is of more general interest and possibly too for new cluster beam deposition techniques [15].

2. MOLECULAR DYNAMICS SIMULATIONS OF 3 AND 5 keV CASCADES IN Cu AND Ni

2.1 Cascade dynamics

MD simulations were employed to study the dynamics and structure of displacement cascades in metals with energies up to 5 keV[9-12]. The primary conclusion of our simulations of cascades in Cu (using the Gibson II potential [7]) and Ni (using a composite

Erginsoy-Johnson potential [16,17]) is that many radiation effects involving displacement cascades can be understood on the basis of two underlying phenomena, replacement collision sequences (RCS's) and local melting. The first, RCS's, are directly responsible for the creation of point defects in the cascade process. This is shown in Fig. 1 where replacement trails leading to the formation of a self interstitial atom (SIA) are indicated. As we will show, the lengths of these RCS's are critically important for determining the number of stable defects that are produced in a cascade. The average length of the RCS's in simulated 3 and 5 keV cascades in Cu (from a total of 46 SIA's) is 23 Å. Despite a determined experimental effort to obtain measured values for RCS lengths, reliable values are notably lacking, thus preventing comparison between simulation and experiment. The only metal for which direct experimental estimates of RCS lengths exists is W [18], and that metal appears to be somewhat atypical [19]. It may turn out that MD simulations will provide the most reliable means to obtain these lengths. In this regard, the question whether RCS lengths and defect production in alloys and compounds are influenced by mass mismatches along the replacement chain arises. Recent MD simulations of defect production in Ni_3Al [20] suggest that the lengths of RCS's are not much influenced by the mass mismatch between Ni and Al but that several configurations of SIA's are produced. Only the smaller Ni atoms, however, are found to form thermally stable SIA's.

The formation of Frenkel pairs by RCS's is not a surprising conclusion of our MD simulations; it was first revealed in the original simulations of Gibson et al. [7]. The second observation of local melting, however, and its profound influence on radiation effects are brought into focus for the first time by our simulations. The possibility of thermal spike behavior in cascades is also not a new concept, having been considered by Seitz and Koehler years ago [4] and by many others since; however, both the precise meaning of a thermal spike and its influence on radiation effects have mostly been a matter of conjecture. The evidence for local melting in the MD simulations derives from various characterizations of the cascade zone. Most visual is a plot of the atomic positions in a cross sectional slab through center of the cascade as shown in Fig. 2a. A disordered zone, which has a rather sharp interface between it and the surrounding ordered matrix, is clearly identified in the center of the cascade. This disordered zone has been characterized by several methods. First, the pair correlation function, g(r), for atoms within this zone was constructed and found to compare closely with that of liquid Cu, Fig. 2b. It was also found that the temperature of this region (temperature is determined using the equation $3/2kT$ = K.E. where k is Boltzmann's constant and K.E. is kinetic energy) was above the melting point of Cu and that the density was approximately that of liquid Cu, i.e. ≈ 10% lower than the solid [10]. Atomic motion was also monitored in this region and it was

found that the diffusion coefficient in this disordered zone was very similar to that of liquid Cu [12]. Because this region looks and behaves like a liquid, we believe it is meaningful and useful to loosely refer to this phenomenon as local melting. We will now show how a variety of radiation effects are naturally explained by the two phenomena of RCS's and local melting. The quantitative results of the MD simulations, of course, do not depend on our qualitative description of local melting.

2.2 Radiation Effects

2.2.1 Defect production: The average number of Frenkel pairs produced in 3 and 5 keV cascades in Cu are 8 and 12, respectively, and 16 in one 5 keV cascade in Ni [10]. These values correspond to defect production efficiencies, with respect to the modified Kinchin-Pease expression, of 0.2 and 0.4 in Cu and Ni, respectively. More recent results of simulation employing EAM potentials rather than pair potentials find similar efficiencies, 0.28 and 0.23 for 5 and 25 keV cascades in Cu [8]. These results that the number of point defects produced in cascades is ≈ 1/3 that predicted by the modified Kinchin-Pease expression agrees well with experimental results on a large number of metals [22]. The reason for the reduced efficiency of defect production in cascades and why it is about the same for most metals has long been puzzling. However, by noting the defect structure in a cascade, a clear picture evolves. The simulations show that all SIA's are located outside the localized region of the cascade that has undergone melting and all of the vacancies lie well within this region. The defect production mechanism can thus be visualized in three steps as shown in Fig. 3. Early in the cascade, SIA's are separated from their nascent vacancies by RCS's. Within the Kinchin-Pease model, all SIA's lying outside the spontaneous recombination volume of a vacancy result in stable Frenkel pairs. In cascades however, the central region undergoes melting and point defect character is quickly lost. Because of the strong repulsive part of potentials at close distances, the local excess density of the SIA's is attenuated sooner than the excess volume of vacancies [23]. As the melt solidifies, therefore, only SIA's outside the melt region and an equal number of vacancies within the core region, remain. Thus, the criterion for a stable Frenkel pair in the Kinchin-Pease model is that the SIA must lie outside the spontaneous recombination volume of the vacancy. In cascades, this criterion becomes that the SIA must lie outside the central melt zone. Defect production in 3 keV cascades in Cu at elevated temperatures has also been investigated with the result that defect production is reduced by a factor of ≈ 3 compared with that at low temperatures [12]. Too few events were simulated to draw a conclusive explanation for the reduction, but we suspect that shorter RCS's and larger melt zones play a dominant role .

2.2.2 Defect Clustering: Calculations of radiation effects at elevated temperatures generally include a source term for migrating defects. On account of defect clustering, only a small fraction of the total number of defects produced generally are free to migrate [24]. Recent experiments have shown that in many metals an important part of the clustering reactions is the formation of vacancy dislocation loops or stacking faults during the cascade evolution [25]. The efficiency for such cascade collapse tends to increase with (i) increasing cascade energy density; (ii) decreasing melting temperature and (iii) increasing irradiation temperature. Although cascade collapse has not yet been directly observed in the MD simulations (mostly because of the low energy events), the simulations do reveal that the vacancies in 5 keV cascades of Cu tend to form tight clusters in the centers of the cascades [10]. The radii of gyration of these clusters are much smaller than that of the locations where the vacancies were first produced. This surprising phenomenon of cascade collapse also finds a natural, although not established, explanation within the local melt model. When the melt zone begins to contract during cooling, the crystal grows nearly perfectly. Because the excess free volume that is left over from the vacancies has a lower free energy in the melt than in the crystal, it tends to accumulate on the liquid side of the solid-melt interface, establishing a free volume gradient in the melt. If the interface velocity is sufficiently slow, the excess free volume can diffuse down its concentration gradient toward the cascade center. This process concentrates free volume in the center of the cascade and establishes the conditions necessary for collapse. If, on the other hand, the interface velocity is too fast, free volume quenches as vacancies in the solid. It is intuitively clear that the interface will move most slowly for materials with low melting temperatures, cascades of high energy density and in lattices at high ambient temperatures. Detailed calculations based on this premise are in progress.

2.2.3 Atomic Mixing: The important role of thermal spikes on ion beam mixing has been established in a number of key experiments [26, 27]. MD simulations of mixing in 5 keV cascade in Cu and Ni is shown in Fig. 4. Here mixing is defined as,

$$\langle R^2 \rangle = 6 \langle D\Delta t \rangle = \Sigma\{\mathbf{r}_i(t = \Delta t) - \mathbf{r}_i(t = 0)\}^2 \qquad (1)$$

where D is the effective diffusion coefficient in the cascade, t is time and the sum is over all atoms in the crystal. At early times in the cascade evolution, $t < 0.15$ ps, mixing in Cu and Ni is very similar. This result is expected since the atomic number, structure and lattice parameter are nearly the same in these two metals and collisional effects dominate this

phase of the cascade development. At later times, however, when the cascade region thermalizes, large differences in mixing between Cu and Ni are seen. We ascribe the greater diffusion in Cu to its lower melting temperature and a longer lasting local melt [28]. This explanation was quantitatively shown to explain the increased mixing with increased Cu or Ag content in a series of irradiated Cu-Ni [29] or Pd-Ag [30] alloys, respectively. The apparent maximum in the mixing curve for Cu in Fig. 4 is an artifact of our definition of mixing (involving means square displacements) which yields a decrease in mixing during the contraction of the melt zone on cooling.

3. MD SIMULATIONS OF HIGH ENERGY CASCADES IN Cu

The MD simulations just described provide a qualitative picture of cascade dynamics, and they provide a physical explanation for various radiation effects. Most experiments, however, have been performed at high energies, making detailed comparison with simulation difficult. Moreover, the simple pair potentials employed for these simulation further complicates detailed comparisons. Recently, however, de la Rubia and Guinan developed an advanced MD code, MOLDYCASK [31], which is based on the Harwell code, MOLDY [32]. This code now makes it possible to simulate cascade events with energies as high as $\approx$ 25 keV in Cu ($\varepsilon = 0.1$ in reduced energy units) and to employ more realistic, isotropic, many-body potentials such as those derived from the embedded atom method [33]. An interesting new result of this work is the elucidation of subcascade formation and the role that local melting plays [8, 31]. Plotted in Fig. 5 are the locations of atoms in a cross sectional slice of a 25 kev cascade at two times, similar to that shown in Fig. 2. Early in the event, the rudiments of subcascade development are seen with two main branches of the cascade evident. At later times, the interconnected subcascades melt into a single, larger entity. These simulations, which use realistic potentials, confirm the idea of local melting and show its importance in subcascade development. From these results, one may expect that for irradiations where the nuclear stopping power is high and the melting temperature of the material low, that an interconnected molten tube is created.

Although detailed analysis of the high energy events has not yet been completed, it is found that [31]: defect production efficiency is $\approx$ 0.25, SIA's are distributed outside the melt region (some in large clusters) and vacancies are clustered in the interior. Cascade collapse was not observed in either of two events. It should be noted, however, that the efficiency of cascade collapse in Cu using 50 keV Kr ions is only $\approx$ 0.3; the efficiency of collapse for self-ions at 25 keV is probably much smaller. Thus, the failure to observe cascade collapse in these simulations is not unexpected. The inward flux of vacancies

during the cascade event is, however, observed as described above. The mixing per unit damage energy in this 25 keV cascade is ≈ 1/2 the experimental value for 1 MeV Kr irradiation of Cu [27] and about twice that for a 5 keV cascade (using EAM potential). From the above considerations of melting, the lower MD than experimental values seem reasonable since we expect that mixing per unit damage energy will increase with energy until subcascade formation is clearly developed, which in Cu occurs at ≈ 50 keV. These simulations thus support the qualitative ideas derived from our previous work. Moreover, they shed light on subcascade formation and are beginning to make more direct comparisons with experiment possible. Once confidence in the quantitative predictions of the simulations is obtained, many phenomenon can be calculated where experimental data are unavailable.

4. ELECTRON-PHONON INTERACTIONS

A natural question that arises in discussions of thermal spikes in metals is whether the electronic system couples to the hot phonon system during the cascade evolution [4,34,35]. Seitz considered this problem using Cu as an example and came to the conclusion that the coupling time between electron and phonon systems is too long for the electronic system to much influence cascade dynamics [4]; Thum and Hofer failed to observed such effects using thermionic emission experiments [33]. This negative conclusion had been widely accepted until recently when it was shown that electron-phonon (e-p) coupling might be important in some metals, albeit, not Cu [36]. The relevant question is whether electrons heat to the phonon temperature while diffusing out of the hot cascade zone, as schematically shown in Fig. 6. Two effects become important if the electrons heat; (i) the heat capacity in some metals becomes comparable to or greater than that of the phonon system so the electrons act as a heat sink, quenching the hot phonon system; (ii) energy acquired by the electrons is transported beyond the cascade boundary by electronic thermal conduction, which is larger than lattice thermal conduction [36]. To determine whether or not electrons heat, we assume that the radius of the hot zone is R and the electron mean free path is λ, then $(R/\lambda)^2$ collisions occur during the random walk. In the one-phonon approximation, an energy $k\theta_D$ is acquired on each collision so that electrons heat to a temperature $T \approx \theta_D(R/\lambda)^2$. The important parameters, therefore, are the cascade radius, the temperature of the spike and the electron mean free path for electron-phonon collisions. The latter is sensitive to the e-p interaction, with metals having high electron densities of states at the Fermi level having the smallest mean free paths (and highest heat capacities). For example, if T = 3000 K, θ_D = 300 K and R = 30 Å, the critical electron mean free path

is ≈ 10 Å. For liquid Cu, λ is ≈ 45 Å [37] so that little coupling is expected, as predicted by Seitz. Experimental values for other metals are not available but calculations yield values of 8, 2.1 and 0.5 Å for Ni, Co and Fe, respectively [38] so that a strong influence of e-p coupling may occur in these metals.

Recently, Caro and Victoria have developed a scheme for including e-p interactions in molecular dynamics codes [39]. Their method uses the Langevin equations of motion, i.e.,

$$M\ddot{\mathbf{x}} = \mathbf{F} + \eta(t) - \beta\dot{\mathbf{x}} \qquad (2)$$

Here, F is the force on an atom described by the interatomic potential. Caro and Victoria show that the electronic excitation can be described in both the electronic stopping power (high velocity) and e-p interaction regimes by a frictional force term of the form $\beta\mathbf{x}$ where β depends only on the local electron density, ρ, in which the moving ion is moving. They suggest the empirical equation,

$$\beta = A \log_{10}(\alpha\rho^{1/3} + b) \qquad (3)$$

where A and a are constants and b is an adjustable parameter which describes the e-p interaction [39]. The local electron density is immediately available in MD codes that use force models based on density-functional formalisms such as EAM. Finally, the term $\eta(t)$ describes the feedback of energy from the hot electrons to the phonon system. This last term is difficult to treat since the electron system is not in equilibrium with itself so that energy transport beyond the cascade boundaries must be determined. This feature, in fact, leads to the surprising result that electrons either couple to the hot phonon system quickly, or almost not at all [36].

Although the above considerations provide a persuasive argument that electron-phonon coupling may play an important role in cascade dynamics, it should be recognized that these models are very approximate, and as yet, no experimental evidence for electron-phonon interactions exists.

5. INTERACTIONS BETWEEN ENERGETIC CLUSTERS AND SOLIDS

The idea of employing energetic clusters of atoms as a means of producing epitaxial thin film growth appears promising since a large quantity of energy can be delivered locally

while each atom in the cluster carries only a very small fraction of the total energy. This differentiates cluster beam deposition from other beam assisted methods where individually accelerated atoms contain sufficient energy to produce radiation damage and to become implanted in the substrate. Consequently, films might be grown at low temperatures since defects and implanted species would need not be annealed out. Although these ideas may seem intuitively clear, they stem from our understanding of individual atom solid interactions and do not consider the effect of many atoms impinging on the surface as a group. Recently discovered cluster fusion [40] demonstrates that cluster-solid interactions can lead to unexpected results. Various regimes of cluster-solid interactions can be identified [41]. At large cluster sizes and low energies, macroscopic models are appropriate, and for small cluster sizes and high energies, the radiation damage theory discussed above can be utilized. For clusters in the range of 10 - 1000 atoms and energies between 0.1 and 5 keV, neither approach is satisfactory and MD simulation again becomes a useful theoretical method.

MD simulations have been carried out for Cu clusters containing 13 or 92 atoms and energies of 325 eV or 1 keV and Cu substrates [42,43]. At this energy, the initial kinetic energy per atom in the larger cluster is equal to the cohesive energy of Cu. EAM potentials were employed in the simulations. Similar to Figs. 2 and 6, the collision dynamics can be illustrated by taking snapshots of the atomic positions in cross sectional slabs at various instants of time, as shown in Fig. 7. The slabs here are of of thickness a_0 (i.e., two (100) planes). Inspection of the figure reveals that the cluster initially depresses the surface rather than penetrating it. Almost immediately ($\approx$ 0.3 ps after contacting the surface), the larger clusters lose their crystalline structure. Maximum compression occurs at $\approx$ 0.7 ps, at which time evidence for plastic deformation becomes evident. As the substrate rebounds, the vibrational energy in the localized region is high and the density is reduced, and some intermixing begins to occur. During this time, original substrate atoms (13 in all) are brought onto the surface at the perimeter of the cluster due to the shear deformation. No evidence is found for local melting of the substrate similar to that observed for the 5 keV cascades. The final configuration of atoms is shown in Fig. 7. Several cluster atoms are embedded in the substrate, some as deep as three atomic planes, but no Frenkel pairs are produced by the cluster. The smaller cluster, for which the energy per atom is 25 eV, the qualitative behavior is quite similar. Due to its smaller projected surface area, the collision exerts a far greater stress on the substrate and accordingly, produces greater deformation. The cluster in this case completely embeds itself in the substrate and leaves a small crater of 6 vacancies above it. Like the larger cluster, substrate atoms are forced onto the surface at the periphery of the cluster and no evidence for substrate melting is observed. The cluster

substrate interaction, therefore, is quite unlike the displacement cascades described above as plastic deformation rather than RCS's and local melting plays the dominant role in the dynamics at these energies. The reason for the absence of local melting is a consequence the low total cluster energy, 325 eV, compared to that in the cascades described above, 3-25 keV. Although 325 eV is sufficient to produce a melt of ≈ 700 atoms, dissipation of heat into the lattice is apparently too rapid for significant melting to occur.

At higher energies, ≈ 1 keV, similar behavior is observed, although the plastic deformation is much greater and local melting begins to become important. This is illustrated in Fig. 7c for the 92-atom cluster. It should also be noted in Fig. 7c that several vacancies are now produced below the surface and many cluster atoms penetrate deeply into the substrate, ≈ 2.5 a_0. It is clear from these simulations that the use of clusters with fewer than ≈ 92 atoms and energies greater than ≈ 1 kev for deposition on substrates with cohesive properties similar to Cu will not produce atomically sharp, defect free, interfaces. It is possible that lower energy clusters, already molten, will provide better deposition conditions, as ≈ 0.5 eV/atom of energy would be added to the thermal energy without change in the momentum of the cluster.

ACKNOWLEDGMENTS

The authors are grateful to several of their colleagues at the University of Illinois and Argonne National Laboratory for helpful suggestions during the development of the ideas presented here. Profs. C.P. Flynn and I.M. Robertson and Dr. W.E. King deserve special mention. The authors are also grateful to Dr. M.W. Guinan for sharing his new MD results with Diaz de la Rubia with us prior to publication. The work was supported by the U.S. Department of Energy, BES, under grants, DE-AC02-76ER01198 and W-31-109-ENG-38 at U.I.U.C. and ANL, respectively. Finally we acknowledge grants of CRAY computer time at MFECC at Livermore, NCSA at U.I.U.C. and the NASA facilities at Ames Research Center.

REFERENCES

1. P. Sigmund, Radiat. Effs. 1, 15 (1969).
2. M.T. Robinson and I.M. Torrens, Phys. Rev. B 9, 5008 (1974).
3. J.P. Biersack and L.G. Haggmark, Nucl. Instr. and Meth. 174, 257 (1980).
4. F. Seitz and J.S. Koehler, in Solid State Physics,, Vol. 2 (Academic Press, New York, 1956) p. 307.
5. G.H. Vineyard, Radiat. Effects, 29, 91 (1976).
6. D. Peak and R.S. Averback, Nucl. Instr. and Meth. B 7/8, 561 (1985).
7. J.B. Gibson, A.N. Goland, M. Milgram and G.H. Vineyard, Phys. Rev. 120, 1229 (1960).
8. T.Diaz de la Rubia and M.W. Guinan, DOE Fusion Technology Bulletin, June, 1990.
9. T. Diaz de la Rubia, R.S. Averback, R. Benedek and W.E. King, Phys. Rev. Lett. 59, 1930 (1987).
10. T. Diaz de la Rubia, R.S. Averback, R. Benedek and H. Hsieh, J. Mater. Res. 4, 579 (1989).
11. T. Diaz de la Rubia, R.S. Averback. R. Benedek and I.M. Robertson, Radiat. Effs. 113, 39 (1990).
12. H. Hsieh, T. Diaz de la Rubia, R.S. Averback and R. Benedek, Phys. Rev. B40, 9986 (1989).
13. see e.g., I. Yamada, H. Taksoka, H. Usui and T. Takagi, J. Vac. Sci Technol. A 4, 722 (1986).
14. see e.g., W.L. Brown , this conference.
15. see e.g., R.P. Andres et al. J. Mater. Res. 4, 704 (1989); Mat. Res. Soc. Symp. Proc. on Clusters and Cluster Assembled Materials (Boston, Dec. 1990) in press.
16. C. Erginsoy, G.H. Vineyard and A. Englert, Phys. Rev. 133, A595 (1964).
17. R.A. Johnson, Phys. Rev. 145, 423 (1966).
18. C.Y. Wei, M.I. Current and D.N. Seidman, Philos Mag. 44, 459 (1981).
19. D.N. Seidman and R.S. Averback, Phys.Stat Solidi, 144, 85 (1987).
20. A. Caro, M. Victoria and R.S. Averback, J. Mater. Res. 5 1409 (1990).
21. S. Foiles, Phys. Rev. B 32, 3409 (1985).
22. P. Jung, J. Nucl. Mater. 117, 70 (1983).
23. T.K. Chaki and J.C.M. Li, Philos. Mag. B 51, 557 (1985).

24. H. Wiedersich, J. Nucl. Mater. (in press).
25. see e.g., J.S. Vetrano, M.W. Bench, I.M. Robertson and M.A. Kirk, Met. Trans. 20A, 2673 (1989).
26. W.L. Johnson, Y.T. Cheng, M. Van Rossum and M-A. Nicolet, Nucl. Instr. and Meth. B7/8, 657 (1985).
27. S.-J.Kim, M-A. Nicolet, R.S. Averback and D. Peak, Phys. Rev. B37, 38 (1988).
28. The mixing in the 5 keV Cu is exaggerated since the melting temperature of the Gibson-II potential is only 1000 K.
29. J.L. Klatt and R.S. Averback, unpublished,
30. J.L. Klatt, R.S. Averback and D. Peak, Appl. Phys. Lett. 55 1295 (1989).
31. T. Diaz de la Rubia and M.W. Guinan, Proc. of the Workshop on Radiation Damage Correlations for Fusion Conditions, Silkeborg, Denmark, 1989; J. Nucl. Mater, in press.
32. M.W. Finnis, Harwell Rept. # AERE-R-13182, 1989.
33. M.S. Daw and M. Baskes, Phys. Rev. B 29, 6443 (1984).
34. F. Thum and W.O. Hofer, Surf. Sci. 90, 331 (1979).
35. Z. Sroubek, Appl. Phys. Lett. 45, 849 (1984).
36. C.P. Flynn and R.S. Averback, Phys. Rev. B38, 7118 (1988).
37. T.E. Faber, in *Physics of Metals, 1. Electrons*, ed. J.M. Ziman (Cambridge at the University, Press, Cambridge 1969) p. 284.
38. J.S. Brown, J. Phys. F. 11, 2099 (1981).
39. A. Caro and M. Victoria, Phys. Rev. A. 40, 2287 (1989).
40. R.J. Buehler, G. Friedlander and L. Friedman, Phys. Rev. Lett. 63, 1292 (1989).
41. C.P. Flynn, unpublished result.
42. Horngming Hsieh and R.S. Averback, Phys. Rev. B42, 5365 (1990).
43. Horngming Hsieh and R.S. Averback, unpublished result.

FIGURE CAPTIONS

1. Lattice sites where atomic replacements have occurred leading to the formation of stable SIA's in 5 keV cascades in Cu.

2. (a) Projection of atom locations in a (100) cross sectional slab of thickness $a_o/2$ near the center of a 5 keV cascade in Cu (from Ref. 9).
   (b) Radial pair correlation functions, g(r), for atoms in the disordered zones of 5 keV cascades in Cu at t = 1.1 ps 3.84 ps (from Ref.9). g(r) for liquid Cu [16] is shown for comparison.

3. Schematic representation of defect production in metals.

4. Atomic mixing in 5 keV cascades in Cu and Ni as a function of time (from ref.10).

5. Projection of atom locations in a (100) cross sectional slab of thickness $a_o/2$ near the center of a 25 keV cascade in Cu. (a) t = 0.29 ps; (b) t = 1.02 ps (from Ref. 8).

6. Schematic diagram of the electron-phonon interaction.

7. Projections of atom locations in a (100) cross sectional slab of thickness a_o near the center of a Cu cluster - Cu substrate collision in: (a) a 92 atom cluster with initial kinetic energy = 325 eV; a 13 atom cluster with initial kinetic energy = 325 eV (from Ref. 42); (c) a 92 atom cluster with initial kinetic energy = 1,000 eV (from Ref. 43).

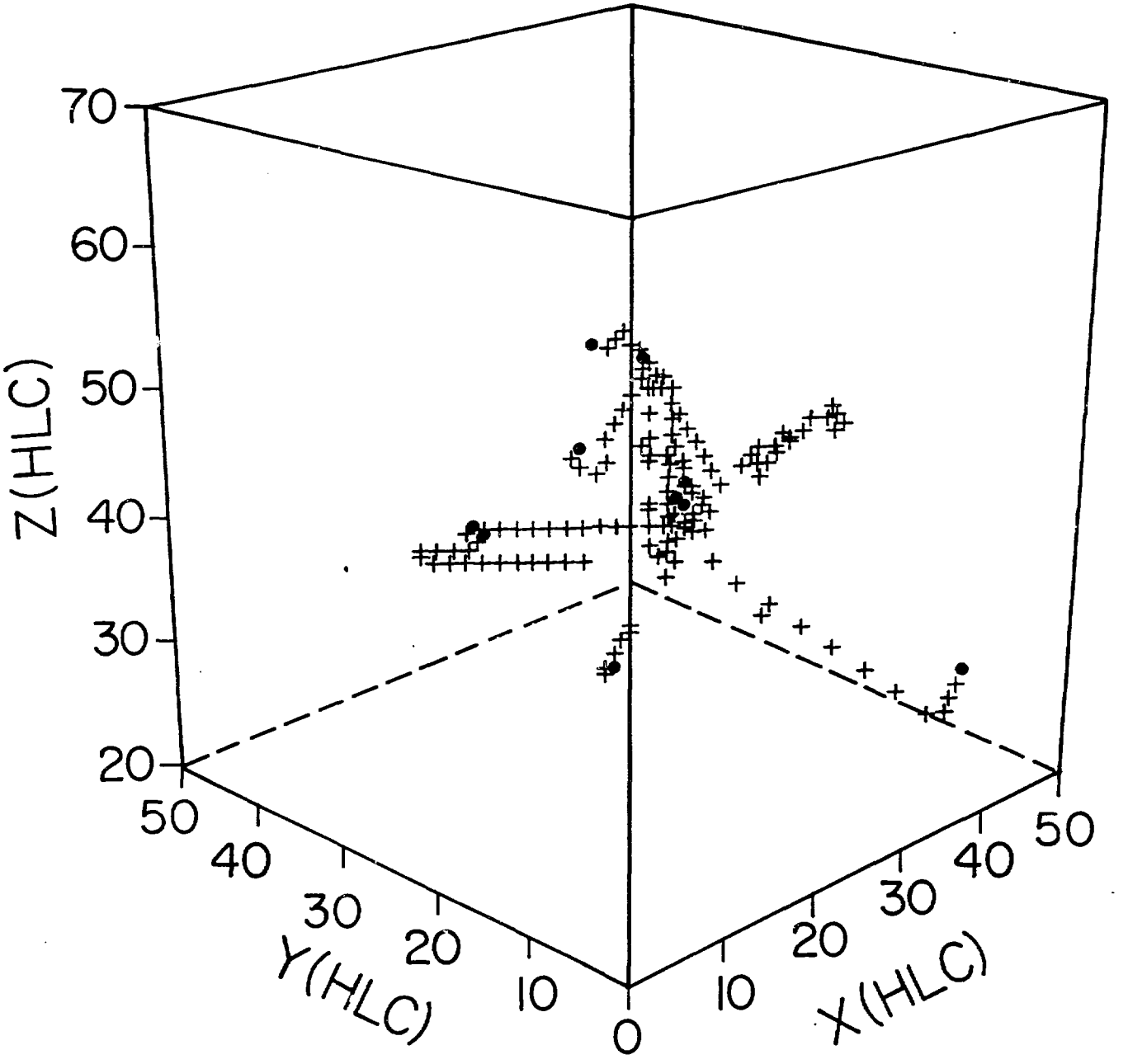
70
60
50
40
30
20
Z(HLC)
50
40
30
20
10
0
Y(HLC)
10
20
30
40
50
X(HLC)

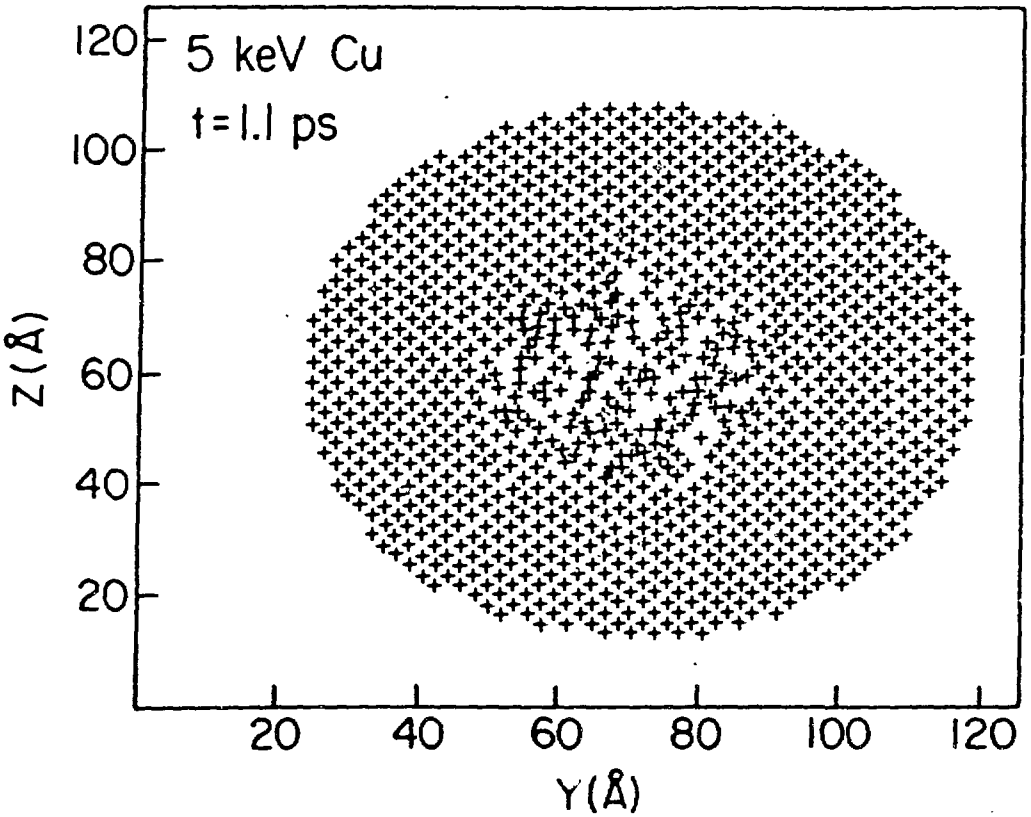
5 keV Cu
t = 1.1 ps
Z(Å)
Y(Å)
120
100
80
60
40
20
20
40
60
80
100
120

2a

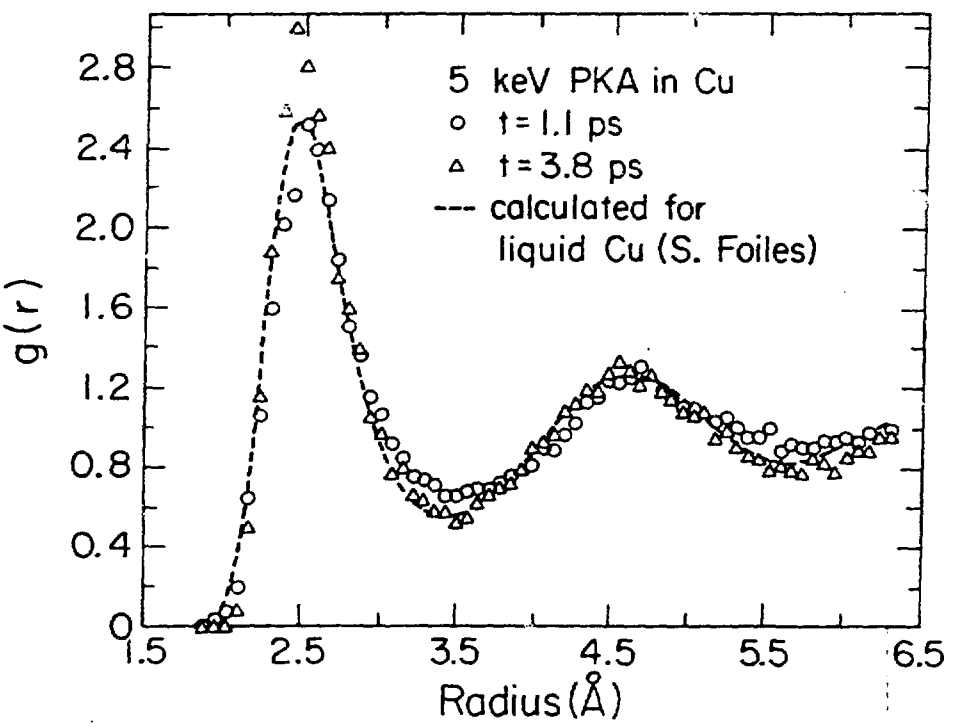
5 keV PKA in Cu
t = 1.1 ps
t = 3.8 ps
--- calculated for
liquid Cu (S. Foiles)
g(r)
Radius(Å)
2.8
2.4
2.0
1.6
1.2
0.8
0.4
0
1.5
2.5
3.5
4.5
5.5
6.5

2b

Figs 2

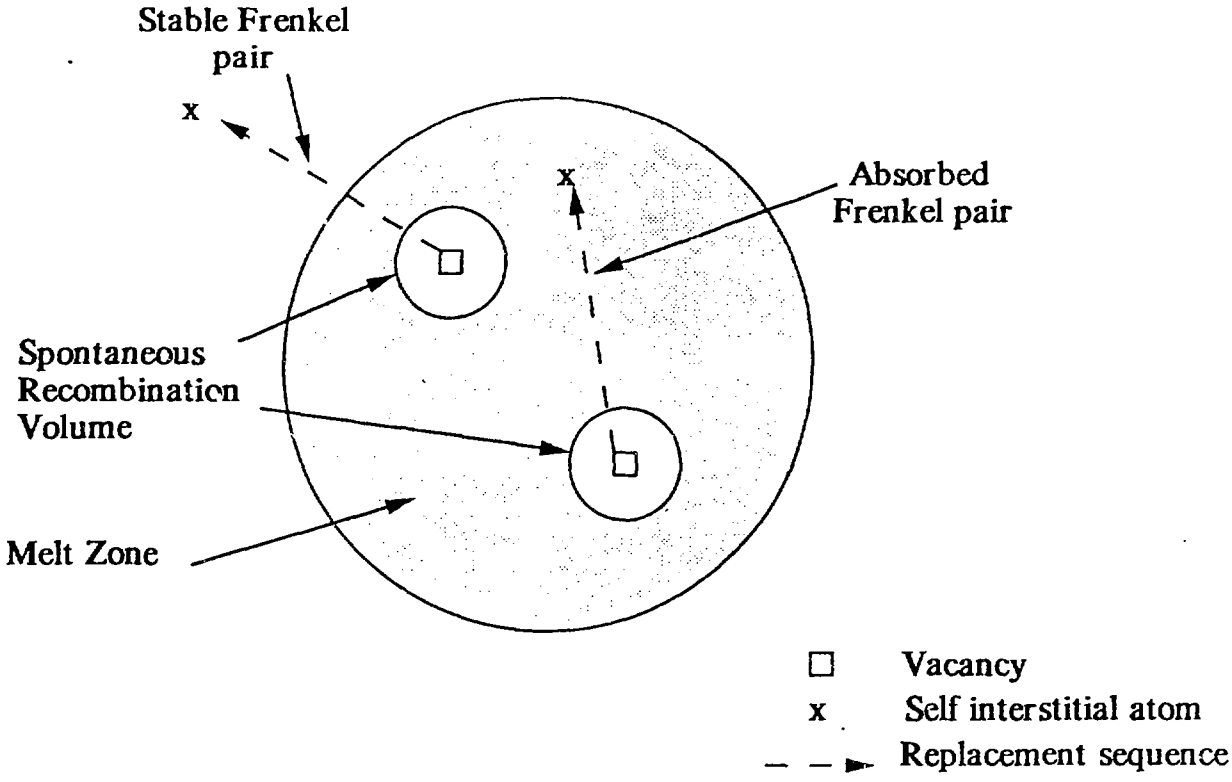
Stable Frenkel pair
x
x
Absorbed Frenkel pair
Spontaneous Recombination Volume
Melt Zone
Vacancy
x Self interstitial atom
Replacement sequence

Fig 3

Fig 3

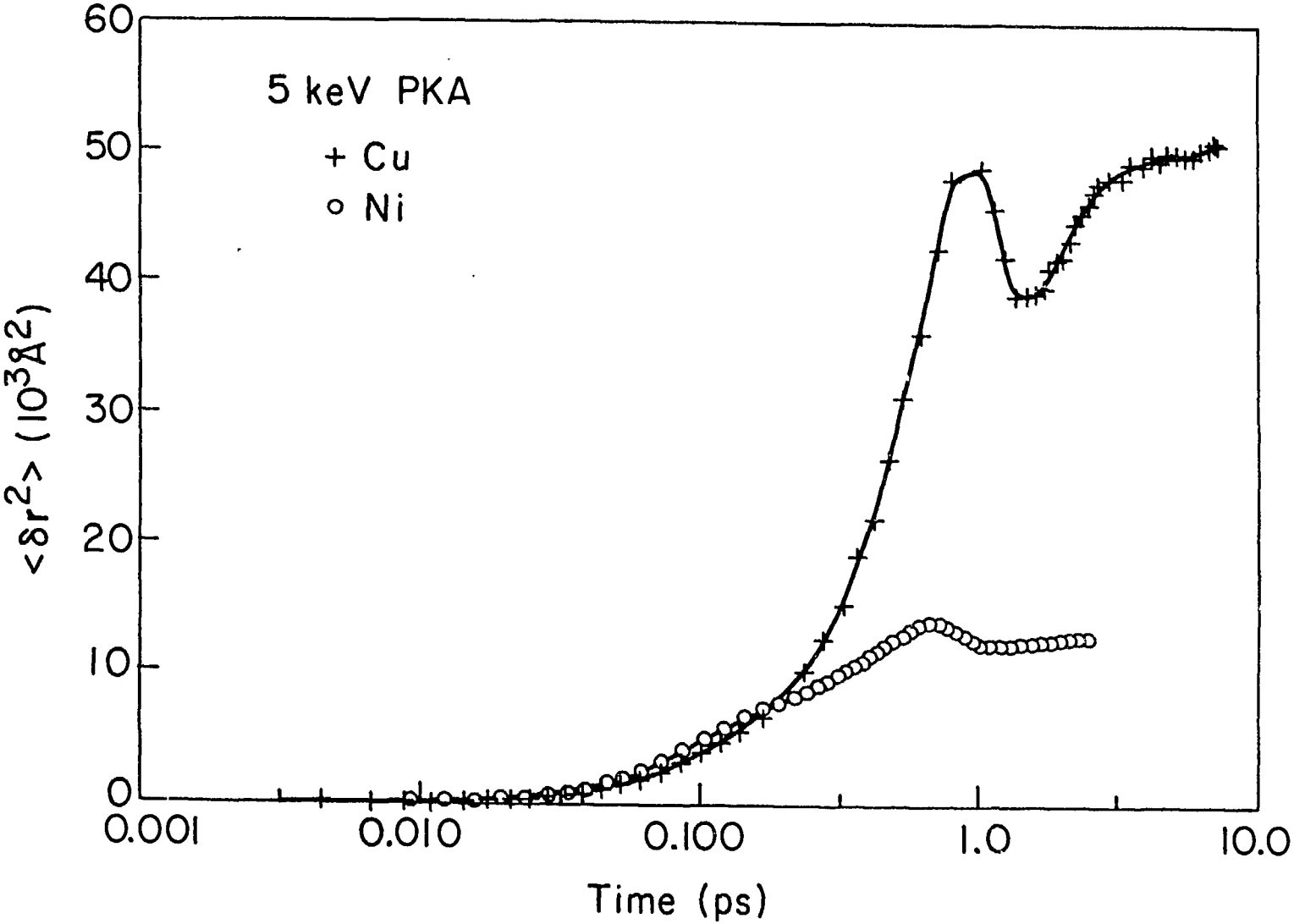
5 keV PKA
+ Cu
o Ni
60
50
40
30
20
10
0
0.001
0.010
0.100
1.0
10.0
Time (ps)
<δr²> (10³Å²)

Fig 4

a)

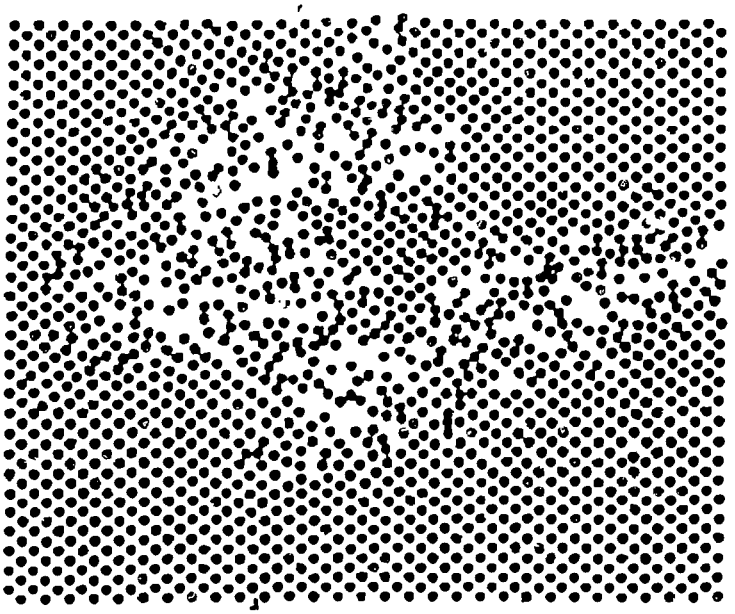

b)

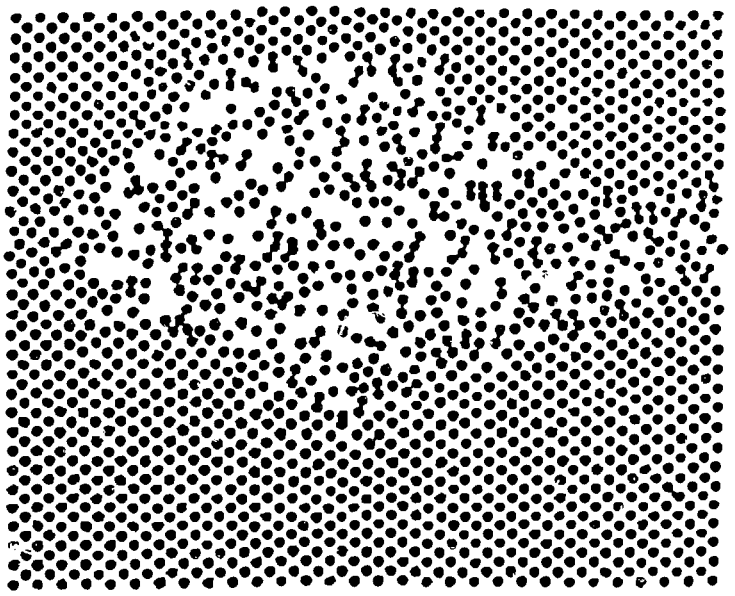

Fig 5

Electron-Phonon Coupling

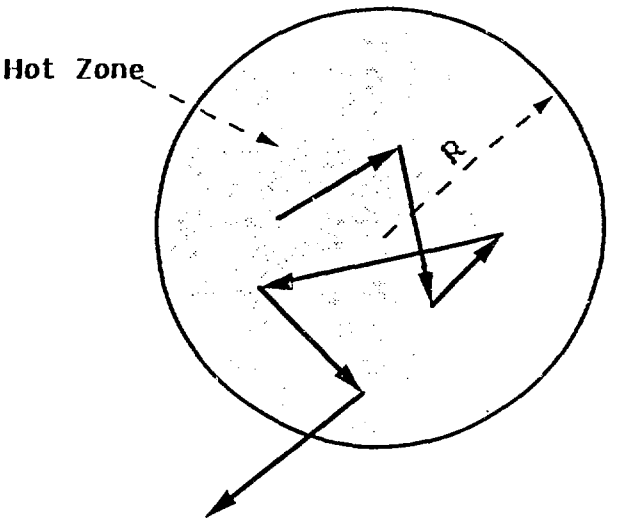

Fig 6

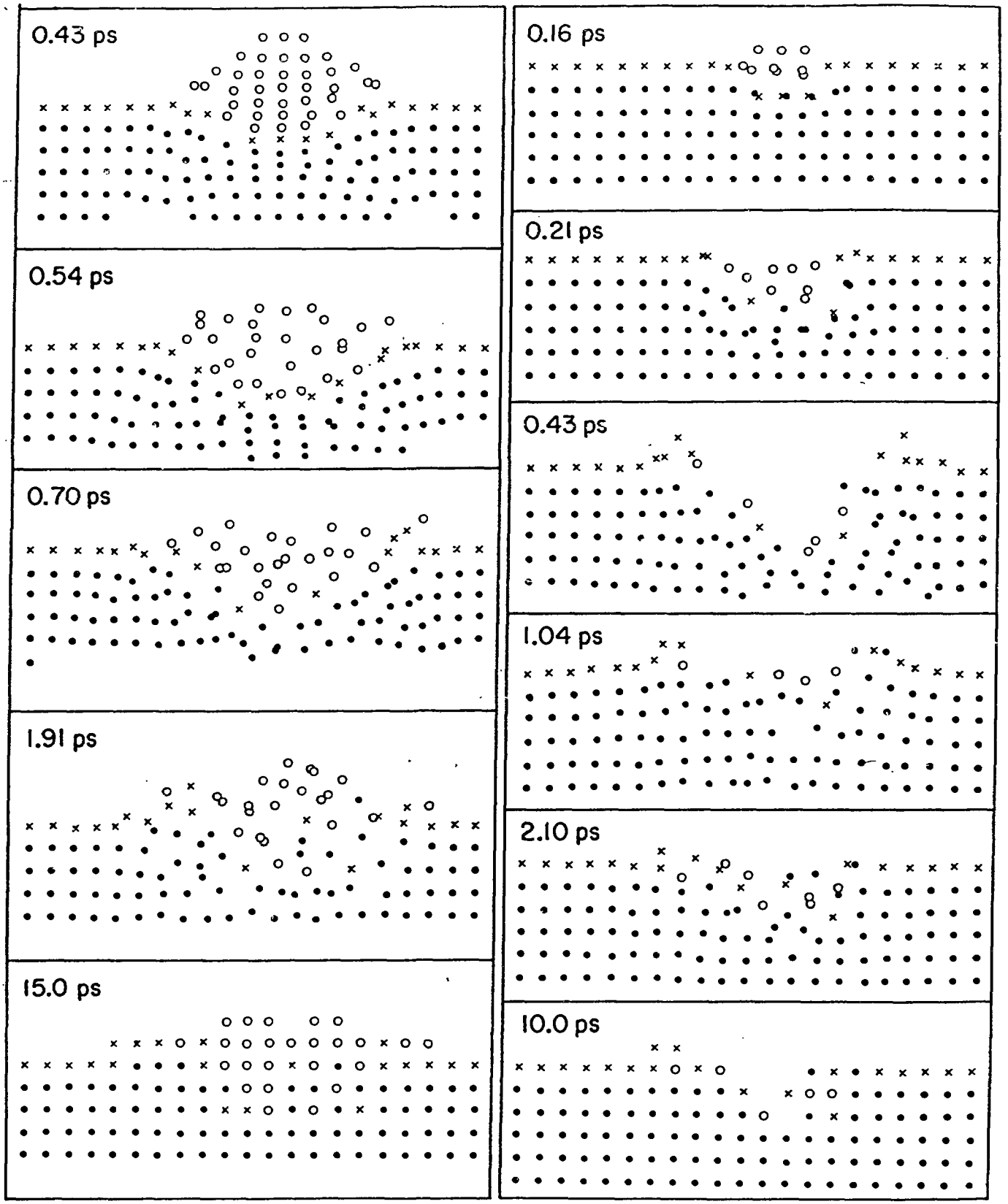
0.43 ps
0.54 ps
0.70 ps
1.91 ps
15.0 ps
0.16 ps
0.21 ps
0.43 ps
1.04 ps
2.10 ps
10.0 ps

Fig 7 (a) (b)

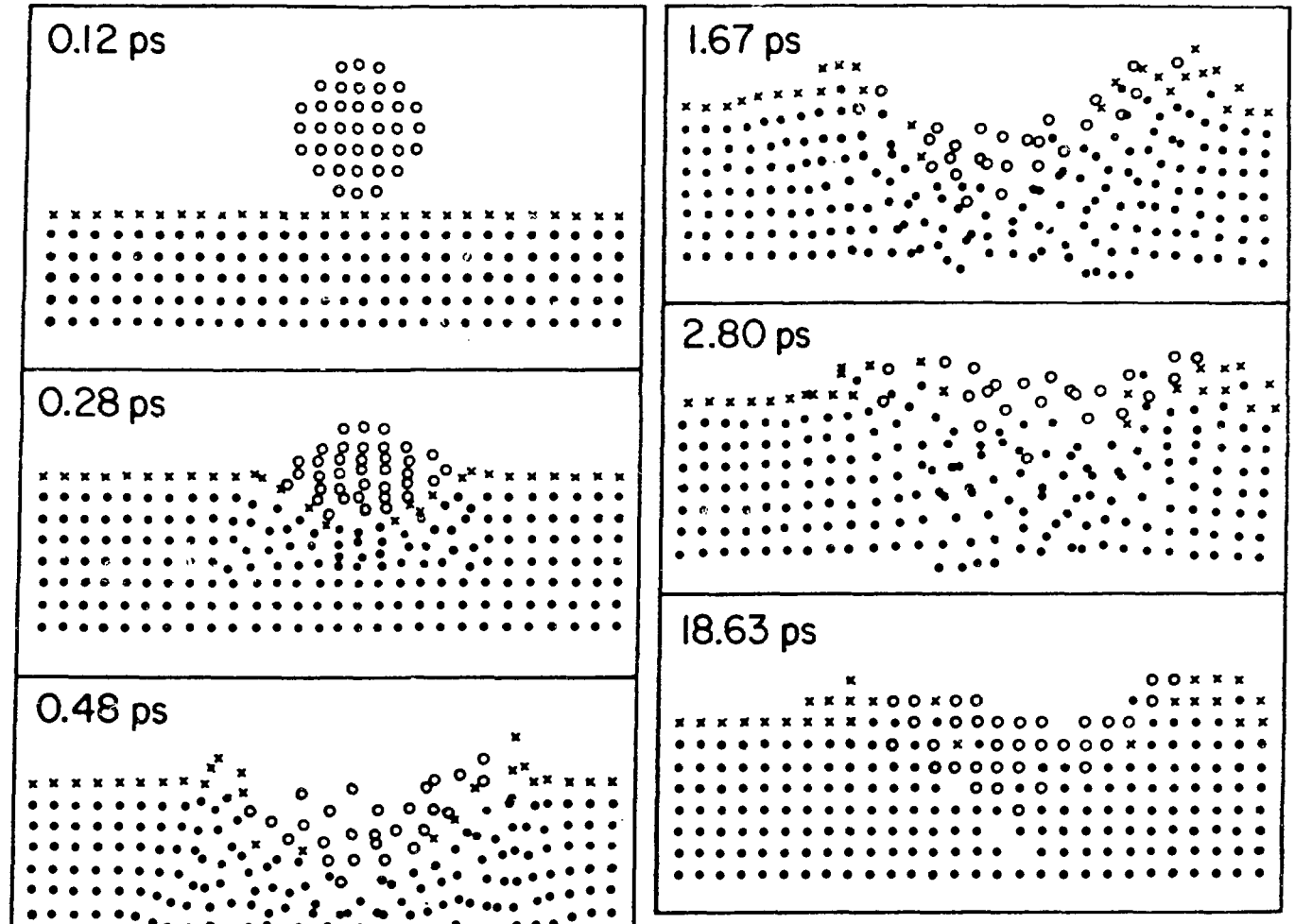

Fig 7c